Available online at www.sciencedirect.com
ScienceDirect
Journal of Power Sources 161 (2006) 524–530
JOURNAL OF POWER SOURCES
www.elsevier.com/locate/jpowsour

Electrochemical storage of hydrogen in nanotubular TiO_2 arrays

P. Pillai, K.S. Raja, M. Misra*

Metallurgical and Material Engineering, University of Nevada, Reno, NV 89557, United States

Received 1 March 2006; received in revised form 30 March 2006; accepted 30 March 2006
Available online 5 June 2006

Abstract

Vertically oriented nanotubular TiO_2 arrays were formed by a simple anodization process. Hydrogen storage studies were carried out on the TiO_2 nanotubular arrays having different diameters by charging and discharging hydrogen with potentiostatic/galvanostatic control. The hydrogen storage capacities of the nanotubes were only marginally affected by the tube diameter. Concentration of oxygen vacancies as defects influenced the hydrogen storage of the nanotubes. Annealing of the TiO_2 nanotubes in argon atmosphere increased the defect density and decreased the hydrogen discharge during initial charge–discharge cycles. Hydrogen storage studies through electrochemical route did not show significant storage capacity of TiO_2 nanotubes. Diffusion of hydrogen as protons and interference of the double layer capacitance of nanotubes could be attributed to the lower hydrogen storage capacity.

Keywords: Nanotubular TiO_2; Hydrogen storage; Cyclic voltammetry; Charge density

1. Introduction

One-dimensional nanostructured materials, such as carbon nanotubes [1], and boron nitride nanotubes [2] are considered for potential hydrogen storage applications. Recently, 2 wt.% of hydrogen storage in TiO_2 nanotubes prepared by hydrothermal process was reported [3]. In the hydrogen storage studies, nanomaterials were used as entangled nanostructures. The larger surface area of the nanomaterials may not be completely utilized when the structure is entangled, as not all the surface areas would be directly exposed to the environment. This problem could be alleviated by the use of aligned or well-ordered nanostructures. Formation of vertically oriented and ordered-TiO_2 nanotubes through a simple anodization process has been reported by several research groups [4,5]. These nanotubes find applications in gas sensing [6], photo-generation of hydrogen [7] and templates for growth of carbon nanotubes [8], nanowires of compound semiconductors and bioceramic coatings [9]. If these nanotubes can store about 2 wt.% hydrogen as reported by Lim et al. [3], which corresponds to about 536 mAh g^{-1} by electrochemical storage capacity, they can find application in metal hydride batteries. The major advantage of the anodization method to prepare nanostructure of TiO_2 is its ability to scale-up. As the nanotubes are vertically oriented and form good electrical contact with the metal substrate, well-controlled functionalization of the nanotubes can be easily achieved. By appropriate cathodic pulsing cycles, the nanotube array can be extracted from the Ti substrate or a thin sputtered layer of Ti can be completely anodized to form a through thickness TiO_2 nanotubular array. This short communication reports the electrochemical hydrogen storage properties of vertically oriented TiO_2 nanotubes prepared by anodization route. The hydrogen storage capacity was investigated as a function of the nanotube diameter. It is well documented that fluoride content and pH are crucial factors for the nanopore formation during anodization. In order to achieve different diameters of the nanotubes, the anodization parameters such as anodization potential, temperature and fluoride content were varied in a pH 2.0 solution.

2. Experimental

Titanium foil (99.9% purity, ESPI Metals, Ashlan, OR, USA) of 0.2 mm thickness was cut into 16 mm diameter blanks and loaded into PTFE holder exposing only 1.0 cm^2 area to the electrolyte. The material was used in as-received condition. The electrolyte was 0.5 M H_3PO_4 + 0.07–0.14 M NaF. The temperature of the anodization was varied from 5–24 °C. Two electrode

* Corresponding author. Tel.: +1 775 784 1603.
E-mail address: Misra@unr.edu (M. Misra).

0378-7753/$ – see front matter © 2006 Elsevier B.V. All rights reserved.
doi:10.1016/j.jpowsour.2006.03.088

configuration was employed. A dc power source (Agilent Technologies) supplied the required potential and current was monitored by a digital multimeter. A flag shaped Pt electrode with about 5 cm^2 surface area was used as a cathode. The distance between the anode and the cathode was about 3 cm. The electrolyte was continuously stirred using a magnetic stirrer. Initially the potential of the Ti sample was ramped from zero to the final anodization potential at a rate of 0.1 $V\,s^{-1}$. During this potential ramp, the current increased. When the potential was maintained constant the current decreased initially and started to increase again. After some time it reached a steady state value. Anodization was continued typically for 20 min after reaching a steady state value. After anodization, the sample was removed from the holder, washed with plenty of distilled water and sonicated in acetone for about 30 s to remove any debris sticking to the surface. The samples were observed under a FESEM (Model S-4700, Hitachi) to determine the morphology and dimensions of the nanotubular structure.

Electrochemical hydrogen storage studies were carried out on the nanotubular TiO_2 samples in as-anodized condition and on selected samples in annealed condition as well. Annealing was carried out in argon flowing atmosphere at 350 °C for 6 h. Three electrode configuration was used for electrochemical studies. The counter electrode was a platinum flag with 5 cm^2 area. Ag/AgCl in saturated KCl acted as a reference electrode. The reference electrode was kept in a Luggin probe filled with saturated KCl solution and sealed with KCl saturated-agar gel. The distance between the TiO_2 sample and the reference electrode was about 3 mm. The electrolyte used for hydrogen charging and discharging was 30 wt.% KOH. The electrolyte was purged with pure nitrogen continuously. In order to evaluate the reduction and oxidation potentials of hydrogen on the nanotubular TiO_2 surface, cyclic voltammetry (CV) studies were carried out. For comparison, as-received (unanodized) Ti sample also was investigated. During the CV, potential was scanned from 1.0 to $-2.3\,V_{Ag/AgCl}$ at two scan rates, 10 and 100 $mV\,s^{-1}$. All the experiments were carried out at room temperature (24 °C) using a computer controlled potentiostat (Model: MSTAT, Arbin Instruments, College Station, TX, USA). Based on the CV results, parameters for hydrogen charging and discharging were selected. Hydrogen charging was carried out by galvanostatic control at different current densities ranging from −0.15 to $-10\,mA\,cm^{-2}$. The charging time varied to reach a total charging capacity of about 1500 $mAh\,g^{-1}$. Discharging was carried out at potentiostatic control ($0.1\,V_{Ag/AgCl}$) as well as galvanostatic control ($1\,mA\,cm^{-2}$). The cut-off potential for charge calculation in galvanostatic experiments was $0.1\,V_{Ag/AgCl}$. Discharging experiments were carried out on un-charged samples also. The charge associated with the potentiostatic/galvanostatic experiments on the un-charged samples was used as a background charge which was not due to oxidation of the hydrogen but current due passivation of the working electrode. In order to calculate the 'true' hydrogen storage capacity of the samples, the background charge was subtracted from the discharge capacity of the 'charged' samples. Ten cycles of charging and discharging were carried out to characterize the hydrogen storage behavior. In this communication all potentials are expressed with reference to Ag/AgCl in saturated KCl whose potential was 0.199 V versus standard hydrogen electrode (SHE).

3. Results and discussion

Fig. 1(a)–(c) illustrates the surface morphologies of the nanotubes with different diameters. It was observed that lowering the anodization temperature did not significantly alter the diameter of the nanotubes. However, nanotubes formed at lower temperatures had thicker walls. Lowering the fluoride content of the electrolyte from 0.14 to 0.07 M was found to affect the diameter of the nanotubes. Decrease in fluoride content decreased the diameter. Further, length of the nanotubes increased with decrease in fluoride content. However, a threshold amount of fluoride was found to be necessary to form nanotubes as anodization in phosphoric acid solution without addition of fluoride did not show any ordered nanostructure [5]. Anodization potential also determined the diameter of the nanotubes. The diameter decreased with decrease in anodization potential. When the potential was below 5 V, no significant nanotube formation could be observed. In this study, nanotubes with three different diameters were investigated, viz., 30, 50, and 100 nm. The anodization conditions for formation of these samples are summarized in Table 1. Formation of nanotubes caused scalloped imprints on the substrate, as shown in Fig. 1(d). The scalloped bottom surfaces of the tubes are inter-connected with each other to form a barrier layer on the Ti substrate.

Fig. 2(a) shows the CV results of nanotubular TiO_2 in 30 wt.% KOH at a scan rate of 10 $mV\,s^{-1}$. In 30 wt.% KOH solution, the redox potential of hydrogen reduction/oxidation can be given approximately as −0.885 V versus standard hydrogen electrode (SHE) or −1.084 V versus Ag/AgCl. Similarly the redox potential for oxygen evolution in 30 wt.% KOH will be 0.345 V versus SHE or 0.146 V versus Ag/AgCl. During the forward sweep (positive to negative potentials, Fig. 2(a)), large anodic current was recorded at potentials more positive than $0.5\,V_{Ag/AgCl}$ and the anodic current continued to flow till the potential reached redox potential of hydrogen reduction. The anodic current could be assigned to oxidation of Ti and not to oxygen evolution. The reason for not considering the oxygen evolution on the TiO_2 surface at this potential region will be discussed later. Till the cathodic potential reached a threshold value, the increase in current was not significant. The abrupt increase in current at potentials more negative to about −1.45 V could be attributed to hydrogen evolution reaction and adsorption of hydrogen on the TiO_2 surface. For effective hydrogen evolution the required cathodic over-potential could be about −0.35 V. When the scan was reversed, a cross-over at −1.55 V could be observed and the current became anodic at more negative potential than the reduction potential of hydrogen. As hydrogen is thermodynamically stable at potentials more negative than its redox potential, the observed anodic current cannot be attributed to the oxidation of hydrogen. As the potentials were cathodic to the initial-open circuit potential of TiO_2, oxidation of Ti may not be the source of anodic current. The anodic current could be attributed to the bulk diffusion of hydrogen in the TiO_2 lattice. Hydrogen adsorbed on the TiO_2 surface could diffuse into the oxide layer.

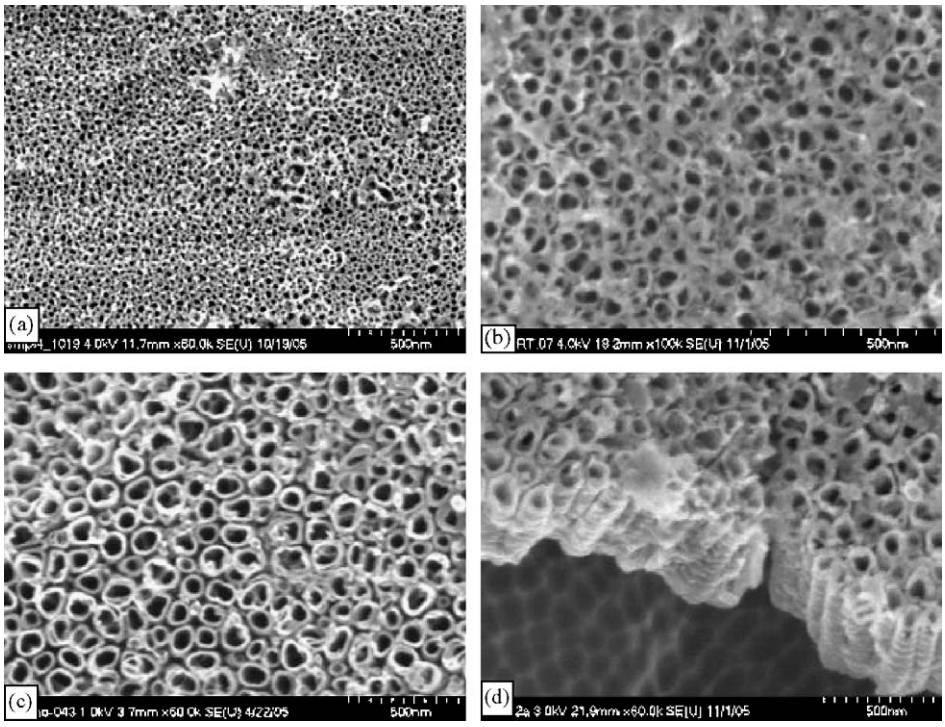

Fig. 1. Morphology of nanotubular arrays of TiO_2 with different diameters: (a) average diameter about 30 nm, (b) 50 nm and (c) 100 nm. Side view of the nanotubes and the scalloped substrate are revealed in (d).

As hydrogen diffused as H^+ ions, the electrons associated with the diffusing hydrogen ions would result in anodic current in the circuit. Further, the anodic current observed at relatively more cathodic potentials could be attributed to the discharging of the double layer. At potentials more positive than −0.4 V, a marginal increase in current could be observed which peaked at about −0.3 V. This current could be attributed to the possible oxidation of adsorbed hydrogen. In order to check that the peak current was not due to mere discharging of the double layer, CV tests were carried out on un-anodized (polished) Ti substrates. In this sample the surface area was much less than that of nanotubular TiO_2 samples. Therefore, the double layer capacitance will be much less. Un-anodized Ti sample also showed an anodic current peak at this potential as seen in Fig. 2(b). It should be noted that the un-anodized sample showed anodic current only at potentials more positive than reduction potential of hydrogen. Therefore, the anodic peaks observed at −0.3 V in both these samples can be attributed to the hydrogen oxidation reaction. The results indicate that a large over potential is required for desorption of hydrogen. This over-potential is much higher than that required for hydrogen evolution. Further, it was observed that the current and over-potential values for hydrogen reduction/oxidation on TiO_2 surface increased with increase in scan rate. The over-potential requirement for nanotubular TiO_2 was higher than that of unanodized Ti surface. Therefore, the potential drop across the thick semiconducting oxide affects the hydrogenation reaction more significantly than the large surface area advantage of the nanostructures.

CV studies were carried out by extending the reverse potential sweep (negative to positive potentials) to more positive potentials till 1.5 V. Increasing the potential in anodic direction did not increase the current during reverse scan. This indicates that oxygen evolution does not occur on TiO_2 surface in the potential range investigated in this study. Sequeira et al. [10] observed oxygen evolution on TiO_2 single crystal surface only above 2.3 V versus SCE in 0.5 M NaOH solution. The higher over voltage required for oxygen evolution on the TiO_2 surface was attributed to the anodic formation of a highly resistant surface layer by the reaction:

$$TiO_{2-x}{\cdot}xOH \rightarrow TiO_2 + xH^+ + xe^- \quad (1)$$

Fig. 3 shows a typical result of potential variations during hydrogen charging of nanotubular TiO_2 sample at $-150\,\mu A\,cm^{-2}$. Open circuit potential before charging was −0.9 V. Impressing cathodic current caused the potential to move in the cathodic direction. Increase in cathodic current density resulted in more

Table 1
Electrochemical conditions for formation of different diameter nanotubes

	30 nm	50 nm	100 nm
Voltage	0–10 V ramping at a scan rate of 0.1 V s^{-1}	0–10 V ramping at a scan rate of 0.1 V s^{-1}	0–20 V ramping at a scan rate of 0.1 V s^{-1}
Concentration	0.07 M NaF + 0.5 M H_3PO_4	0.14 M NaF + 0.5 M H_3PO_4	0.14 M NaF + 0.5 M H_3PO_4
Temperature	Room temperature (24 °C)	Room temperature (24 °C)	Room temperature (24 °C)

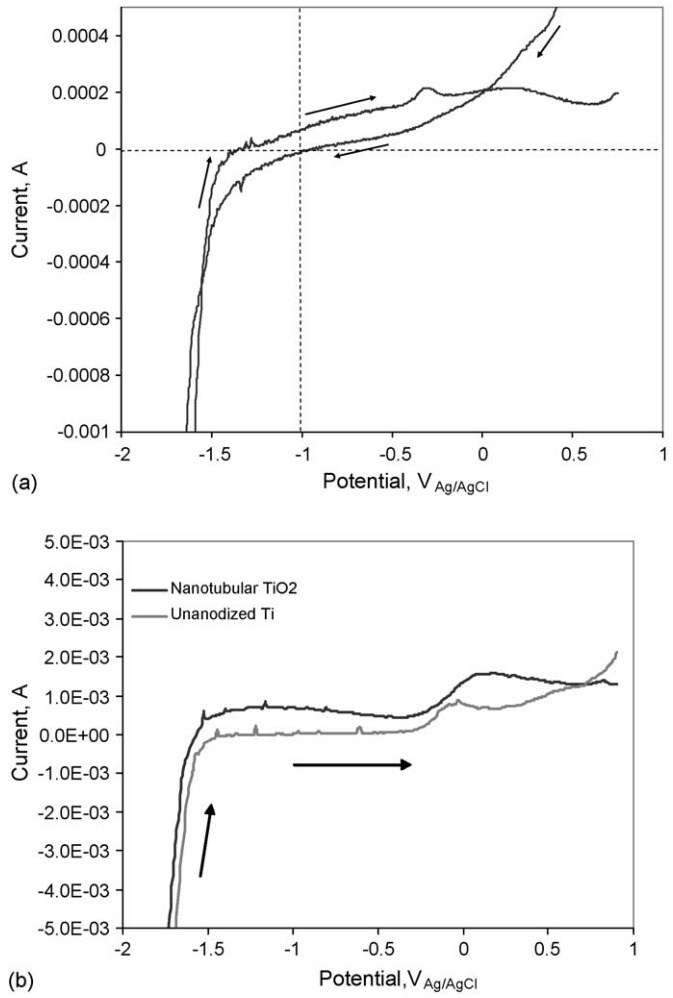

Fig. 2. (a) Cyclic voltammogram of nanotubular TiO_2 (anodized Ti) sample in 30 wt.% KOH. The initial scan was from positive to negative direction at a rate of 10 mV s^{-1}. (b) Cyclic voltammogram of nanotubular TiO_2 and un-anodized Ti in 30 wt.% KOH. The scan rate was 100 mV s^{-1}. Only the reverse potential scan from −2.3 to 1.0 V is shown.

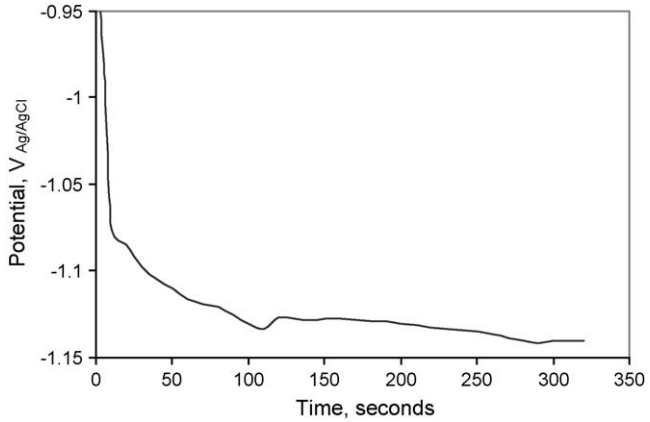

Fig. 3. Potential variation of TiO_2 nanotube arrays (100 nm diameter) when charged with −150 μA cm^{-2} current density in 30 wt.% KOH solution.

negative potentials. For example, application of −150 μA cm^{-2} resulted in a steady state potential of about −1.14 V and at −10 mA cm^{-2}, the potential was −1.82 V. When the charging was interrupted the potential moved in anodic direction. Application of 0.1 V resulted in anodic current corresponding to desorption and oxidation of the hydrogen. Fig. 4(a) shows a typical current behavior at potentiostatic discharge of the previously hydrogen charged specimen. Fig. 4(b) shows the current decay behavior of an uncharged (which was not charged with hydrogen by cathodic polarization) nanotubular TiO_2 polarized with 0.1 V constant potential. The charge associated with this polarization was considered as background charge for passivation. This charge was subtracted from the discharge capacity of the charged samples (for example, charge calculated from Fig. 4(a)) to calculate the 'true' charge associated with hydrogen desorption and oxidation. Fig. 4(c) shows the potential variation during a galvanostatic discharge. A potential plateau could be observed during initial period for about 300 s and the potential started increasing in the anodic direction. During hydrogen desorption, a well-defined potential plateau is expected. Whereas, increase in potential (as observed in Fig. 4(c)) indicates a psuedo-capacitance behavior. This result indicates that the large surface area of the nanotubes function predominantly as a capacitor rather than sites for hydrogen adsorption. Table 2 summarizes the true hydrogen storage capacities of the nanotubular samples with different diameters. It should be noted that all the samples contained Ti substrate in addition to the TiO_2 nanotubes. However, these values were corrected by the background charge values, which also contained component from the Ti substrate. Therefore, the capacity values represent the storage values of TiO_2 nanotubes only. In the calculation only the theoretical mass of the TiO_2 nanotubes were considered. The mass of the nanotubes were calculated based on their geometry and theoretical density of anatase TiO_2.

From the results of hydrogen charge–discharge cycle experiments carried out on the TiO_2 nanotubes in 30 wt.% KOH solution the following observations can be made: increase in charging current density did not alter the storage capacity of 100 nm diameter of the nanotubes. The storage capacity decreased with increase in number of charge–discharge cycles and almost stabilized after fifth cycle. The hydrogen storage capacity increased when the diameter of the nanotubes was decreased to 50 nm. However, further decrease in diameter to 30 nm gave almost same storage capacity as that of 50 nm diameter tube. Therefore, a relation between the diameter and the storage capacity was not clearly established. The hydrogen storage capacity did not vary with the diameter for the annealed samples. As compared to the as-anodized samples, the annealed samples showed lower capacity during first cycle and the stabilized storage capacity during subsequent cycles was similar to that of the annealed sample.

When cathodically charged, the hydrogen enters as positively charged ion into the TiO_2 surface according to the following reaction step:

$$H_{ad} \rightarrow H^+ + e^- \quad (2)$$

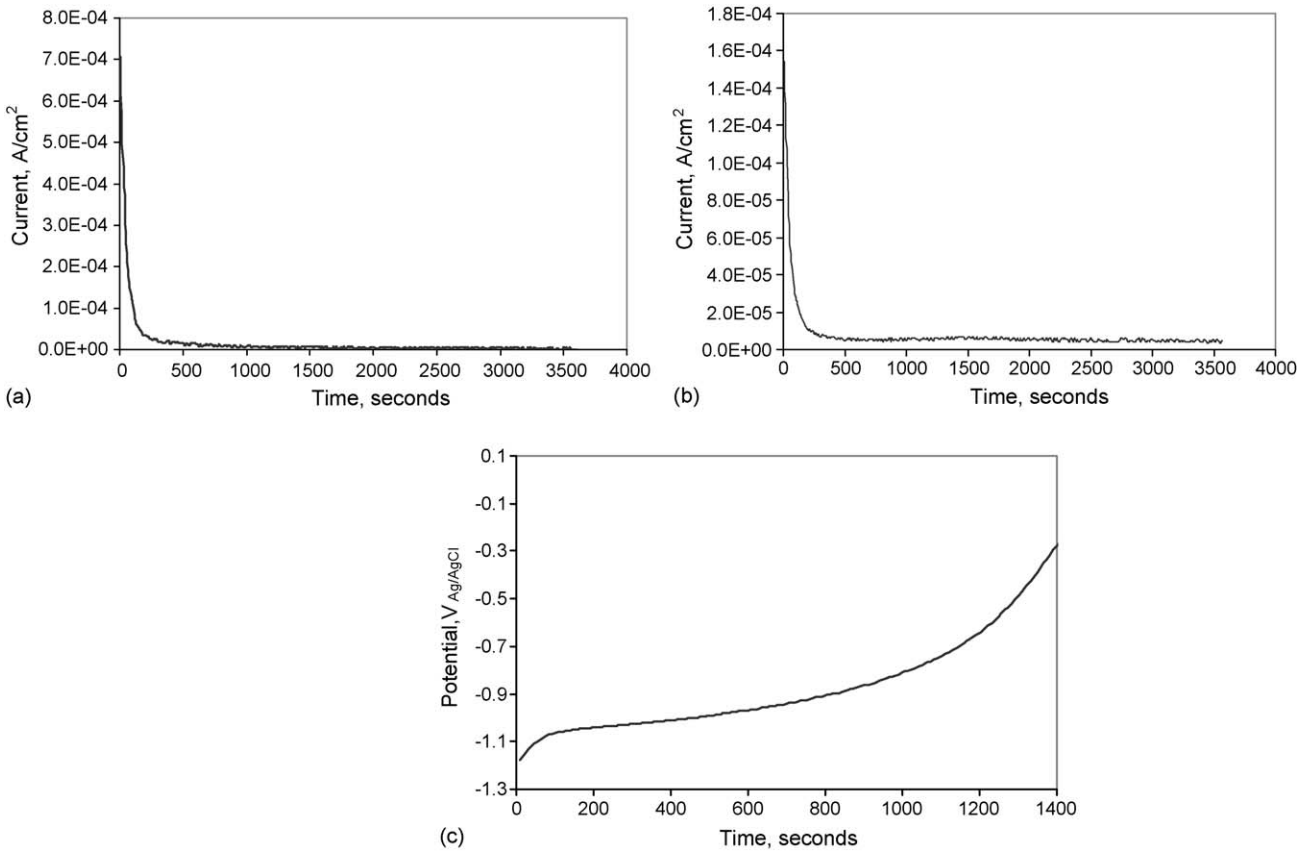

Fig. 4. (a) Current variation during potentiostatic (at 0.1 V) discharge cycle of TiO_2 nanotubes previously hydrogen charged at $-0.75\,mA\,cm^{-2}$. (b) Current transient of uncharged TiO_2 nanotubes when potentiostatically polarized at 0.1 V. The charge accumulated during this potentiostatic control is considered as background charge of the nanotubes for hydrogen storage capacity calculations. (c) Potential variation during galvanostatic ($1\,mA\,cm^{-2}$) discharge of hydrogen from TiO_2 nanotubes previously charged with hydrogen at a current density of $-1\,mA\,cm^{-2}$.

The electrons produced in the above reaction could reduce the Ti^{4+} ion in the TiO_2 to Ti^{3+} and the H^+ ion is associated with O^{2-} ion. As O–H bond is considered to be stronger than the metal–hydrogen bond, conversions of $Ti^{4+} \rightarrow Ti^{3+}$ and $O^{2-} \rightarrow OH^-$ are considered to be more feasible hydrogen storage mechanisms [11]. The alternate mechanism [12] of hydrogenation could be heterolytic cleavage of hydrogen into H^+ and H^- and equilibration of these ions with Ti^{4+} and O^{2-} respectively as Ti^{4+}/H^- and H^+/O^{2-}. Occurrence of this type of hydrogenation with TiO_2 will be rare, because of weak M–H bonds and for electro-neutrality O^{2-} should be converted into O^-. However, these reactions have been proposed for non-reducible type oxides such as MgO [13]. At the surface, permeation of hydrogen is electric field assisted because of electron accumulated space charge layers. As the hydrogen enters the oxide film as a proton, after crossing the space charge layer the transportation is controlled by concentration gradient and diffusivity. Yoon and Pyun [14] determined the diffusivity of hydrogen in polycrystalline anatase thin film to be 3.4×10^{-11} to $1.7 \times 10^{-10}\,cm^2\,s^{-1}$ depending on the charging potential. As the TiO_2 is hydrogenated as O–H surface bond, higher O–H bond strength and lower diffusivity of hydrogen in TiO_2 make the hydrogen desorption kinetics very slow. During discharge, the following reaction is proposed to result in anodic current at lower anodic potentials:

$$TiO_{2-x}{\cdot}xOH \rightarrow TiO_2 + xH^+ + xe^- \quad (3)$$

It is observed that the above reaction required large value of over potential because of stronger O–H bonds in TiO_2.

The final hydrogen storage capacity of the nanotubular TiO_2 was in the range of 3–5 $mAh\,g^{-1}$ which is very low as compared to the 2 wt.% (about $536\,mAh\,g^{-1}$) storage capacity reported for hydrothermal processed TiO_2 nanotubes by dry gas charging method. The reason for such low storage capacity could be attributed to the very low density of the reversible traps of the nanotubes employed in this investigation. During dry-gas charging the large surface area of the TiO_2 nanotubes would be effectively involved in physisorption of hydrogen. In aqueous solution hydrogen charging, the surface area effect would be offset by the presence of double layer. Therefore, hydrogen storage occurs by bulk diffusion of hydrogen in the TiO_2 lattice as H^+ protons. Considering the nanotubular structure as non-stoichiometric TiO_2, the defect density will influence the hydrogen storage capacity. In order to estimate the defect density of TiO_2 nanotubes and its effect on hydrogen storage capacity, Mott–Schottky analysis was carried out on the as-anodized and annealed nanotubular samples. Fig. 5 shows

Table 2
Summary of hydrogen storage capacity of TiO_2 nanotube arrays having different diameters as a function of charging and discharging conditions and number of cycles

Charging and discharging condition	Hydrogen storage capacity ($mAh\,g^{-1}$)		
	100 nm nanotubes	50 nm nanotubes	30 nm nanotubes
−150 μA and 0.1 V			
Cycle #1	26.37	38.00	34.47
Cycle #5	4.12	14.97	9.91
Cycle #10	3.22	6.37	6.35
−750 μA and 0.1 V			
Cycle #1	37.64		
Cycle #5	3.84		
Cycle #10	2.48		
−15 μA and 0.1 V			
Cycle #1	23.00		
−10 mA and 0.1 V			
Cycle #1	16.48		
Cycle #5	4.36		
Cycle #10	3.1		
−10 mA and 1 mA			
Cycle #1	8.26		
Cycle #5	5.22		
Cycle #10	3.24		
−150 μA and 0.1 V TiO_2 annealed in argon atmosphere at 350 °C for 6 h			
Cycle #1	8.60	9.41	
Cycle #5	3.44	4.03	
Cycle #10	2.12	3.21	
−150 μA and 0.1 V TiO_2 annealed in oxygen atmosphere at 350 °C for 6 h			
Cycle #1	12.8		
Cycle #5	7.4		
Cycle #10	4.4		

a typical Mott–Schottky result of 30 nm diameter nanotubular arrays in 30 wt.% KOH solution. The slope of the plot was used for calculating the defect density using the well-known Mott–Schottky relation [15]. Table 3 summarizes the defect density of the specimens. Annealing in argon atmosphere was

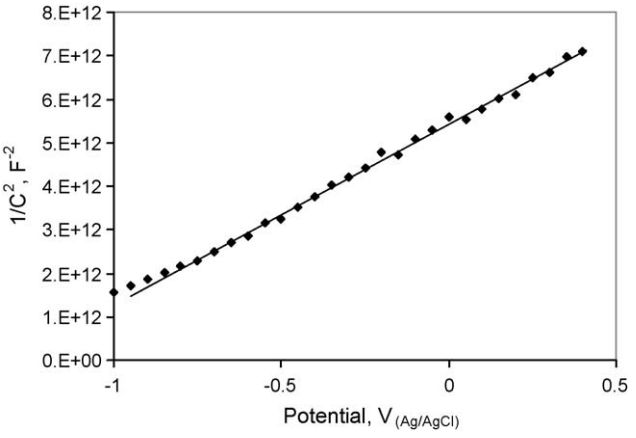

Fig. 5. Mott–Schottky plot of 30 nm diameter TiO_2 nanotubular arrays in 30 wt.% KOH solution. The slope of the linear region was considered for defect density calculation.

Table 3
Defect densities of nanotubular TiO_2 specimens

Specimen	Defect density (cm^{-3})
100 nm diameter TiO_2, as-anodized	1.2×10^{17}
100 nm diameter TiO_2, annealed in argon	1.7×10^{19}
100 nm diameter TiO_2, annealed in oxygen	5.3×10^{15}
30 nm diameter TiO_2, as-anodized	5.1×10^{16}

observed to increase the defect density, whereas annealing in oxygen atmosphere decreased the defect density. As the TiO_2 nanotubes showed n-type semiconductivity, the defects in the lattice are considered as oxygen vacancies. Therefore, it is reasonable to assume that annealing in low oxygen partial pressure (in this case, argon atmosphere) increased the oxygen vacancy in the material. As oxygen vacancies are positively charged, these defect sites cannot be traps for hydrogen in the nanotubes. Therefore, increase in defect density of the annealed sample reduced the hydrogen storage capacity significantly, especially during first charge–discharge cycle. Similarly, marginal increase in storage capacity of the smaller diameter nanotubes could be attributed to the lower defect density. However, annealing in oxygen atmosphere did not improve the storage capacity significantly as compared to that of argon-annealed specimens. Therefore, in addition to the method of gas charging, the method of formation of TiO_2 nanotubes also could affect the storage capacity. In hydrothermal processing, TiO_2 nanotubes were formed by rolling of titanate sheets. According to Chen et al. [16], the nanotubes formed by alkali hydrothermal treatment were trititanate, having $H_2Ti_3O_7$ structure. The trititanate is a monoclinic phase, constructed by corrugated sheets of edge-sharing TiO_6 octahedra [17]. Whereas, TiO_2 nanotubes formed by anodization show predominantly an amorphous structure in as-anodized condition and transform to tetragonal anatase phase after low temperature (350 °C) heat treatment [18]. However, Lim et al. [3] claimed that the hydro thermally prepared material was pure TiO_2 and the layer-structured titanates such as $Na_2Ti_3O_7$ could only be intermediate products. If $Na_2Ti_3O_7$ were present, this would increase the hydrogen storage capacity by replacing the Na^+ cations with H^+. In this present study, no effort was made to measure the hydrogen storage capacity of the hydro thermally prepared TiO_2 (or trititanate) nanotubes using electrochemical method.

As the nanotubes were vertically oriented, they had easy access to adsorption of hydrogen and desorption as well. In fact this behavior has been effectively used for hydrogen gas sensing applications [6]. Even though the TiO_2 nanotube arrays did not show encouraging results as a promising hydrogen storage material by electrochemical technique, it should be quickly pointed out that, in combination with other nanostructured materials, a better hydrogen storage characteristic could be obtained. For example, Lueking and Yang [19] observed that metal oxides incorporated on the carbon nanotubes (CNTs) enhance the hydrogen storage by about 40%. TiO_2 nanotube arrays can be used as templates for growth of CNTs and the composite structure of CNT + nanotubular TiO_2 could result in enhanced hydrogen storage. In fact, preliminary studies carried

out in our laboratory on the CNT + nanotubular TiO_2 arrays composite structure showed interesting results which will be reported elsewhere. Future work will include measurement of the hydrogen storage capacity using dry-gas charging method.

4. Conclusions

- Electrochemical hydrogen storage studies were carried out on different diameter TiO_2 nanotubular arrays using 30 wt.% KOH electrolyte at room temperature.
- A simple anodization procedure was employed to form the vertically oriented arrays of nanotubes. Variation of the diameter of the nanotubes was obtained by modulating the anodization potential and electrolyte chemistry.
- The hydrogen storage capacity was marginally affected by the diameter of the nanotubes.
- The defect densities of TiO_2 nanotubes influenced the hydrogen storage capacity.
- Annealing of TiO_2 nanotubes in argon atmosphere increased the defect density and decreased the storage capacity during initial charge–discharge cycles. The steady state storage capacity was not altered by the heat treatment.
- Nanotubular TiO_2 arrays did not show significant hydrogen storage capacity through electrochemical route because of two reasons: (1) hydrogen diffused as protons and (2) the large surface area of the nanostructure acted more as an interfacial capacitor than adsorption sites for hydrogen.

Acknowledgement

This work was sponsored by U.S. Department of Energy through DOE Grant No. DE-FC52-98NV13492. The authors gratefully acknowledge the financial support of DOE. The authors thank Mr. Gautam Priyadharshan and Dr. Mo Ahmedian for their assistance in the experimental work.

References

[1] A.C. Dillon, K.M. Jones, T.A. Bekkedahl, C.H. Kiang, D.S. Bethune, M.J. Heben, Nature 386 (1997) 377.
[2] T. Oku, M. Kuno, I. Narita, J. Phys. Chem. Solids 65 (2004) 549.
[3] S.-H. Lim, J. Luo, Z. Zhong, W. Ji, J. Lin, Inorg. Chem. 44 (2005) 4124–4126.
[4] J.M. Macak, H. Tsuchiya, P. Schmuki, Angew. Chem. Int. Ed. 44 (2005).
[5] K.S. Raja, M. Misra, K. Paramguru, Electroch. Acta 51 (2005) 154–165.
[6] O.K. Varghese, D. Gong, M. Paulose, K.G. Ong, C.A. Grimes, Sens. Actuators B 93 (2003) 338–344.
[7] J.H. Park, S. Kim, A.J. Bard, Nanoletters 6 (2006) 24–28.
[8] M. Misra, K. Paramguru, P. Pillai, K. S. Raja, Mater. Lett., communicated.
[9] K.S. Raja, M. Misra, K. Paramguru, Mater. Lett. 59 (2005) 2137–2141.
[10] C.A.C. Sequeira, J.P. Joseph, J.M.B. Fernandes Diniz, Solid State Ionics 26 (1988) 197–201.
[11] A. Fahmi, C. Minot, Surf. Sci. 304 (1994) 343.
[12] L.L. Knotek, Surf. Sci. 91 (1980) L17.
[13] J. Leconte, A. Markovits, M.K. Skalli, C. Minot, A. Belmajdoub, Surf. Sci. 497 (2002) 194–204.
[14] Y.-G. Yoon, S.-I. Pyun, Electrochim. Acta 40 (1995) 999–1004.
[15] F. Di Quarto, M. Santamaria, Corros. Eng. Sci. Technol. 39 (2004) 71–81.
[16] Q. Chen, W. Zhou, G. Du, L.-M. Peng, Adv. Mater. 14 (2002) 1208–1211.
[17] R. Ma, Y. Bando, T. Sasaki, Chem. Phys. Lett. 380 (2003) 577–582.
[18] O.K. Varghese, D. Gong, M. Paulose, C.A. Grimes, E.C. Dickey, J. Mater. Res. 18 (2003) 156–165.
[19] A. Lueking, R.T. Yang, J. Catal. 206 (2002).